9th Asia-Pacific Conference on Wind Engineering
Auckland, New Zealand
3-7 December 2017

Flutter Derivatives of a Thin Plate Model under Different Attack Angles

Qi Wang[12], Yulin Li[2] , Haili Liao[12] and Yuxuan Yan[2]

[1]Department of Bridge Engineering
Southwest Jiaotong University, Chengdu 610031, China

[2]Research Centre for Wind Engineering
Southwest Jiaotong University, Chengdu 610031, China

Abstract

It was widely studied that the flutter derivatives of a thin plate under 0° wind attack angle, whereas the derivatives under different wind attack angle are rarely recognized. Using a thin plate model with 40 side radio as an object, the flutter derivatives was tested under 0°, 3°, 5°, 7° by forced vibration tests. It was shown that the four important flutter derivatives of a thin plate are consistent with the ones of an ideal thin plate. The flutter derivatives A_2* were negative under 0°, 3°, 5°, whereas were positive under 7° wind attack angle when the reduced wind speed is greater than 8, and its absolute value decreased with the attack angle increasing. The changes of other flutter derivatives were not obviously than A_2* under 0°, 3° , 5° , but were significant under 7° wind attack angle. The flutter critical wind speeds were calculated by coupled flutter close-form solution and obtained directly by free vibration wind tunnel tests. The error between the two results is less than 5% which proved the validity of the flutter derivative. The research achievements can be benefit to the analysis of flutter of long span bridges with the effect of wind attack angle.

Introduction

Scanlan [1] proposed the flutter derivatives of bridge deck to describe the motion-induced aerodynamic force, and also provide a method to identify the flutter derivatives. Shinozuk [2] proposed a method to identify the flutter derivatives by using ARMA model in time domain. Diana [3] report a test to obtain the flutter derivatives via full-scale aero-elastic model. The accuracy of the identifications can be verified by the flutter derivatives of a thin plate since it has the analytical values. Actually, a thin plate with a definite thickness in wind tunnel tests is not an ideal thin plate with zero-thickness, and its flutter derivatives only can be close to the ideal ones. Noda [4] studied on the effect of amplitudes on flutter derivatives of a thin plate with side ratio 200 using pressure testing. However, the effect of attack angle on flutter derivatives of a thin plate has not been reported ever. As a result, this paper studied on the flutter derivative of a thin plate with side ratio 40 under different attack angles. The flutter derivative obtained by forced vibration and verified by free vibration wind tunnel test. The results indicated that, the flutter onset speeds obtained by using the flutter derivatives to calculate and the ones obtained from the free vibration testing are very close to each other.

Test setup

Forced Vibration Test

Flat plate model adopted by the test is 1.1m long, 0.4m wide, 0.01m thick and ratio of width to height 40:1, which meets the size of thin flat plate in the engineering significance. In order to reduce its own inertia forces and ensure stiffness, the model is made of carbon fiber so that its mass is only 2.2 kg. Wind tunnel testing of forced vibration is proceed in No.1 wind tunnel of Southwest Jiaotong University. The forced motion of the model is carried out by means of four direct current motors mounted on the floor united drive. Four actuators of the device are equipped with displacement sensors and force sensors to synchronously collect the force and displacement in the wind axes coordinate system. In the course of testing, the device's front actuator and the plate are connected to 1, 2 points (shown in Fig.1), the distance from the centre of the model is 145mm; the rear actuator and the plate are connected to 3, 4 points (shown in Fig.1), the centre of model.

Four force transducers and four acceleration sensors all adopt the low-pass filter with cut-off frequency of 30Hz. When the wind velocity is U, the force of the four actuator is f_1, f_2, f_3, f_4 respectively. Therefore, the total vertical lift L and torsion moment M are:

$$L = f_1 + f_2 + f_3 + f_4 \tag{1}$$

$$M = \left(f_1 + f_2 \right) * 0.145 \tag{2}$$

The forced vibration device drives the model with single-degree-of-freedom vertical vibration and single-degree-of-freedom torsional vibration at 0°,3°,5° and 7° angle of attack to obtain the motion-induced aerodynamic force under different conditions. According to the existing literature on flutter derivatives of flat plate under forced vibration, the amplitude of vertical vibration is set to 10 mm, the amplitude of torsional vibration is 2°, and vibration frequency is 2.5 Hz, reduced velocities range from 4 to 18. To ensure the flow in two dimensions, a rigid plate of size 600mm×200mm×6mm is fixed at the end of the model and parallel to the inflow of wind tunnel. The test equipment and model installed in the wind tunnel are shown in Fig. 2.

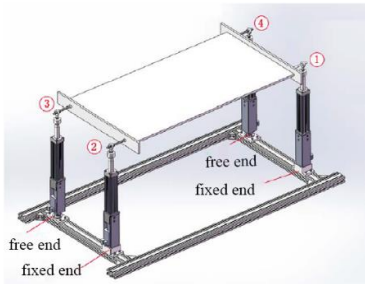

Fig.1 Details of the forced vibration device

Fig.2 Wind tunnel test of forced vibration

Data Processing

The expression of vertical and torsional motion of single-degree-of-freedom is as follows:

$$h(t) = h_0 \sin(\omega_h t) \tag{3}$$

$$\alpha(t) = \alpha_0 \sin(\omega_p t) \tag{4}$$

where h_0 is the amplitude of heaving motion, ω_h is the corresponding angular frequency; α_0 is the amplitude of torsional movement, ω_p is its angular frequency. When the vertical excitation occurs, No.1~4 actuators move synchronously; when the torsional excitation occurs, No.3 and No.4 actuators remain stationary, No.1 and No.2 actuators move synchronously.

According to flutter derivatives expressions [1], the lift force and moment can be written as follows:

$$L_{se}(t) = \frac{1}{2}\rho U^2 (2b)(kH_1^* \frac{\dot{h}}{U} + kH_2^* \frac{b\dot{\alpha}}{U} + k^2 H_3^* \alpha + k^2 H_4^* \frac{h}{U}) \tag{5}$$

$$M_{se}(t) = \frac{1}{2}\rho U^2 (2b^2)(kA_1^* \frac{\dot{h}}{U} + kA_2^* \frac{b\dot{\alpha}}{U} + k^2 A_3^* \alpha + k^2 A_4^* \frac{h}{U}) \tag{6}$$

where ρ is air density, U is wind velocity, b is the half width of sectional model, The reduction frequency is $k = \omega b/U$, H_i^* and $A_i^*(i = 1,2,3,4)$ are the dimensionless function of k, known as flutter derivative or pneumatic derivative.

Based on the above expression (1) ~ (6), after derivation the expression of eight flutter derivatives under the single-degree-of-freedom condition are as follows:

$$H_1^* = \frac{C_{LH}}{h_{r0}k^2}\sin(\phi_{LH} - \varphi_H) \tag{7}$$

$$H_2^* = \frac{C_{LP}}{\alpha_0 k^2}\sin(\phi_{LP} - \varphi_P) \tag{8}$$

$$H_3^* = \frac{C_{LP}}{\alpha_0 k^2}\cos(\phi_{LP} - \varphi_P) \tag{9}$$

$$H_4^* = \frac{C_{LH}}{h_{r0}k^2}\cos(\phi_{LH} - \varphi_H) \tag{10}$$

$$A_1^* = \frac{C_{MH}}{h_{r0}k^2}\sin(\psi_{MH} - \varphi_H) \tag{11}$$

$$A_2^* = \frac{C_{MP}}{\alpha_0 k^2}\sin(\psi_{MP} - \varphi_P) \tag{12}$$

$$A_3^* = \frac{C_{MP}}{\alpha_0 k^2}\cos(\psi_{MP} - \varphi_P) \tag{13}$$

$$A_4^* = \frac{C_{MH}}{h_{r0}k^2}\cos(\psi_{MH} - \varphi_H) \tag{14}$$

where $H_i^*(i = 1\sim4)$ is the flutter derivative related to lift force; C_{LH} is lift coefficient generated by heaving motion, $\emptyset_{LH}$ is the correspondng phase angle; C_{LP} is lift coefficient generated by torsional movement, $\emptyset_{LP}$ is the corresponding phase angle; φ_H and φ_P are the phase angle between the aerodynamic forces at the same time in the heaving motion and torsional movement respectively. C_{MH} is moment coefficient generated by heaving motion ψ_{MH} is the corresponding phase angle; C_{MH} is moment coefficient generated by heaving motion, ψ_{MH} is the corresponding phase angle; C_{MP} is moment coefficient generated by torsional movement, ψ_{MP} is the corresponding phase angle; k is the reduction frequency, α_0 is the amplitude of torsional movement, h_{r0} is the reduction amplitude of heaving motion, which is obtained as $h_{r0} = h_0/b$, b is the half width of the model.

Free vibration Tests

In order to verify the accuracy of the flutter derivative measured by the forced vibration device, the free vibration flutter test is designed to obtain the actual flutter wind velocity of the same model at different wind angles of attack, and then compare it with the flutter wind velocity calculated from the flutter derivative. Wind tunnel testing of free vibration was conducted in No.2 wind tunnel of Southwest Jiaotong University. Wind angle of attack is still adjusted to 0°, 3°, 5° and 7°. Using the traditional system sectional model with spring suspension, as shown in Fig. 3. In the test, the dynamic characteristics of the system vibration are changed by adjusting the spacing of the springs, the spacing of the mass, to obtain the corresponding flutter wind velocity of the model.

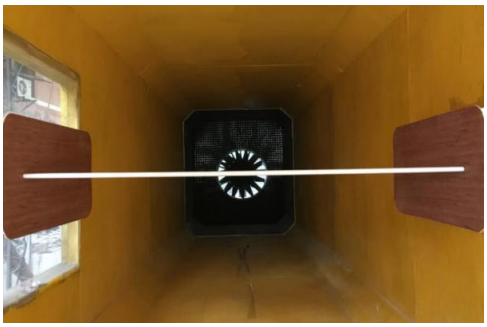

Fig. 3 Wind tunnel test of free vibration

Calculation of Critical Flutter Velocity

The calculation of the critical flutter wind velocity is given by Chen [5] who proposed the formula of closed solution of the double-modal coupled flutter. This formula can be used to calculate the flutter factor γ by using the flutter derivatives, which can quantify the variation of the flutter property of different sections with reduction wind velocity at different wind angles of attack. It deserves noting that, since the formula can only calculate the critical wind speed of the coupling flutter (A_2^* is negative at this time), then for the positive value of A_2^* (+7° wind angle of attack), the calculation of the critical wind velocity of the flutter is based on the two-degree-of-freedom step-by-step flutter calculation method proposed by Matsumoto[24].

The expression of the double-modal coupled flutter closed solution is as follows:

$$U_{cr} = \gamma \omega_{s2} b \sqrt{\left(1 - \frac{\omega_{s1}^2}{\omega_{s2}^2}\right)\frac{mr}{\rho b^3}} \tag{15}$$

where U_{cr} is critical flutter wind velocity, ω_{s1} and ω_{s2} are the angular frequency of vertical and torsional motion respectively, b is the half width of the bridge section, m is equivalent mass per unit length of the main girder, r is the inertia radius of the equivalent mass, $\rho = 1.225\, Kg/m^3$ is air density. γ is the flutter factor, expressed by the following formula:

$$\gamma = 1/\sqrt{F_1 + F_2} \tag{16}$$

$$F_1 = (r/b)\mathrm{D}^2(-k^2 H_3^*)(kA_1^*)/[(-kA_2^*) + 2k\xi_{s2}(1 + \upsilon A_3^*)^{\frac{1}{2}}/\upsilon] \tag{17}$$

$$F_2 = (b/r)(k^2 A_3^*) \tag{18}$$

where $k = \omega b/U$ is the reduced frequency of the half-bridge width, ξ_{s2} is structural damping ratio of torsional movement; $\upsilon = \rho b^4/I$, I is equivalent mass moment of inertia of unit

length. A_1^*,A_2^*,A_3^*,H_3^* are pneumatic derivatives. D is the factor that characterizes the similarity of the vibration mode of bending and torsion, with the sectional model test D=1.0

Test Results of Flutter Derivative

Attack Angle: zero degree

Firstly, the forced vibration device drives the thin plate under the angle of 0° with single-degree-of-freedom vertical and torsional movement respectively, and the displacement and feedback force time-history of four actuators are obtained. Through calculating by the formula (9) ~ (16) can obtain eight flutter derivatives, as shown in Fig.4. The results of the test show that, the four flutter derivatives A_1^*, A_2^*, A_3^*, H_3^*, which play a dominant role in calculating the critical flutter wind velocity, are basically in accordance with the theoretical solution of the ideal plate. The slight differences are: the three derivatives related to the aerodynamic damping, A_1^*, A_2^* and H_3^*, are slightly greater than the value of the ideal plate; A_3^* is almost exactly to theoretical value. The other four noncritical derivatives in addition to H_1^* are different from the theoretical values, whose absolute value are greater than the theoretical value of the ideal plate.

Attack Angle: non-zero degree

Adjust the absolute displacement of No.1 and No.2 actuators so that the thin plate is at the attack angle of 3°, 5° and 7° respectively. The model is derived to single-degree-of-freedom vertical and torsional movement respectively. Eight flutter derivatives at different angles of attack obtained by testing are shown in Fig.5. The test results show that, with the increase in the angle of attack, A_2^* decreases gradually. At +5° angle of attack, it is negative but close to zero; at +7° attack angle, when the reduced wind velocity is less than 8, its negative but close to zero, and when the reduced wind speed is greater than 8, it becomes positive. This indicates that A_2^* from negative to positive in the process of the wind attack angle from + 5° to + 7°, can also be considered in the change of the average wind angle, the flat from the streamlined to blunt body. The absolute value of the coupling derivative H_3^* also increases with the increase of the angle of attack, indicating that the coupled negative damping increases with the angle of attack. The coupling flutter derivative A_1^* increases with the increase of the attack angle between 0° and + 5°; when the angle of attack is + 7°, the angle of A_1^* is significantly reduced, even less than the value of 0° attack angle, indicating that the vertical movement of blunt body generated by the coupling of aerodynamic benefits is weaker than the streamline.

The change trend of aerodynamic stiff term A_3^* is similar to the change of the A_1^* value. When the reduced wind velocity of the thin plate is less than 12, the value of A_3^* at the four kinds of attack angle is closer; when the reduced wind velocity is greater than 12, the value of A_3^* at +5° and +7° angle of attack are less than at 0°, and the value at +7° is less than the value at +5°. For the flutter derivatives H_1^* and H_4^*, the absolute value increases with the increase of the angle of attack in the range of 0° to +7°, and is negative. The value of A_4^* increases with the increase of the angle of attack in the range of 0° to +5°; when the angle of attack is +7°, the value of A_4^* is converted from positive to negative. The value of H_2^* increases with increasing angle of attack, and significantly increased at +7°.

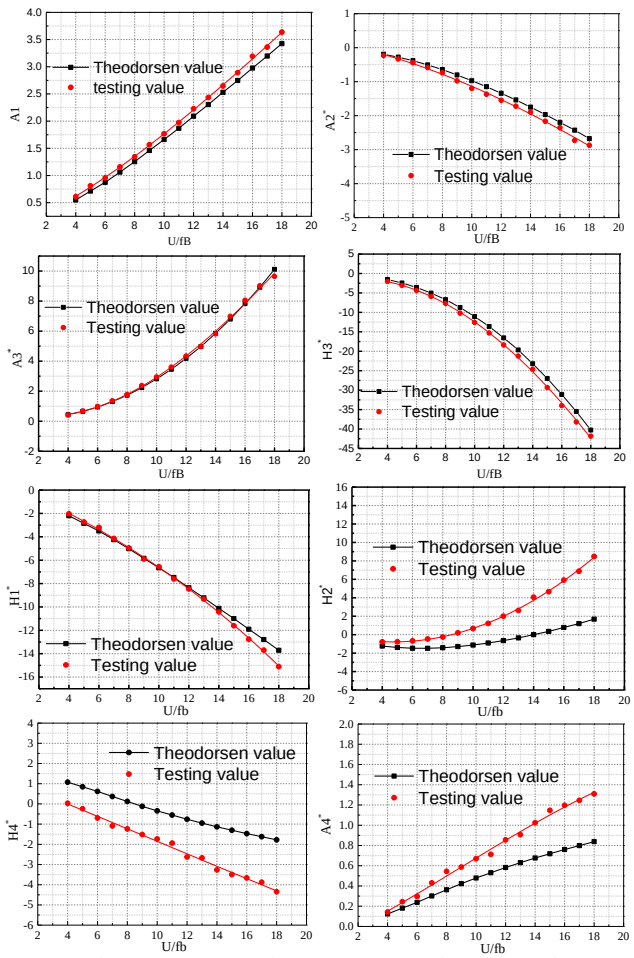

Fig.4 The flutter derivatives of thin plate(angle of attack: 0°, frequency 2.5Hz, vertical amplitude 10mm, torsional amplitude 2°)

Verification of Flutter Derivatives

In order to verify the accuracy of flutter derivatives at different attack angles measured by forced vibration method, the flutter critical wind velocity obtained by the free vibration test, and then by means of the formula (15) can back-calculate the flutter factor under each condition. The parameters and results of each test case are shown in Table 1. The test results show that, the critical wind velocity of the flutter is significantly reduced as the attack angle increases from 0° to 7°, the increment of the attack angle and the decrement of the wind velocity are nonlinearly related. At 0° and 3° attack angle, ratios of bending and torsion, radius of inertia and torsional frequency change significantly, and the range of the flutter reduced wind velocity is wide (from 6 to 12). However, the value of the flutter factor remains stable at an average of 0.416 (empirical coefficient in the Selberg formula), as the flutter property of the plate is only affected by flutter derivatives instead of affected by the reduced wind velocity. At 5° and 7° attack angle, the flutter factor has a large dispersion while the range of the flutter reduced wind velocity is narrow (range from 5.78 to 8.55 at 5° changed 2.77, range from 4.68 to 5.47 at 7° changed less than 1). Since flutter derivatives are hardly affected by the reduced wind velocity at this time, and the flutter derivative and the dynamic parameters have dual effects on the flutter factor, the fixed flutter derivative cannot be adopted to quantify the flutter property of the plate under different conditions.

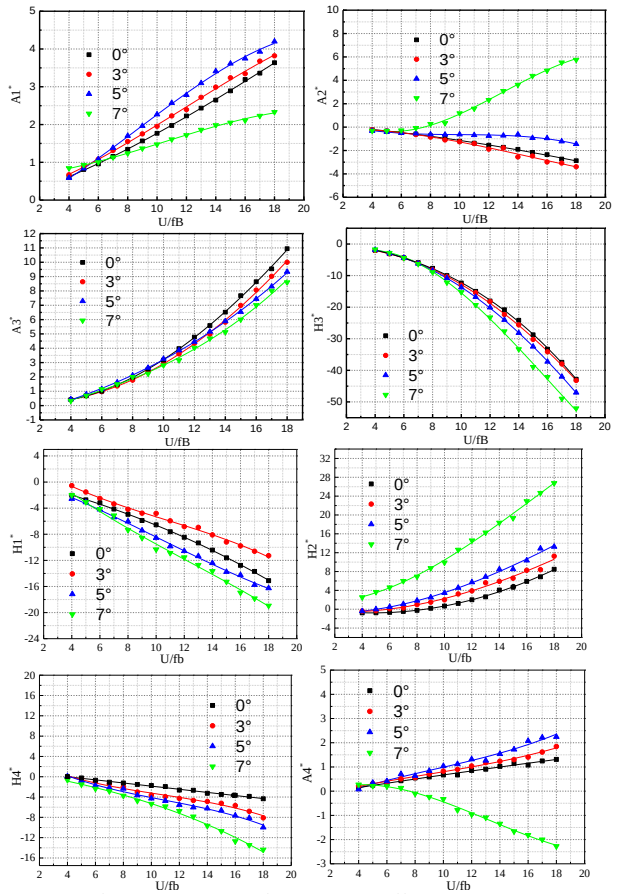

Fig. 5 The flutter derivatives of thin plate at different wind attack angles(0°, 3°, 5°, 7°)

Testing Case	r/b	f_t	f_t/f_h
case 1	0.720	2.68	1.14
case 2	0.828	3.26	1.39
case 3	0.916	3.77	1.61

Table 1. The test results of free vibration

In order to verify the accuracy of flutter derivatives, the program of critical wind velocity of two-dimensional flutter and the dynamic parameters corresponding to test conditions are calculated to obtain the theoretical flutter reduced wind velocity for each test condition, and the calculated results are compared with the flutter reduced wind velocity obtained by wind tunnel testing, as shown in Table 2. It can be seen that the error of flutter reduced wind velocity for calculation and experiment is within 4.5% under all cases, which verifies the accuracy of the measured flutter derivative at different angles of attack in this paper.

Conclusions

By taking the thin flat plate with side ratio 40 as the research object, the forced vibration and free vibration wind tunnel test are adopted to carry out testing the flutter derivatives and flutter critical wind velocity at 0°, 3°, 5° and 7° attack angle, main conclusions are as follows:

(1) The four dominant flutter derivatives of the thin plate model and the ideal plate are consistent. The other derivatives are different from the theoretical values except H_1^*.

(2) The flutter derivative A_2^* is negative at 0°, 3° and 5° attack angle as well as decreases with the increase attack angles. At 7° angle of attack, when the reduced wind velocity is less than eight, A_2^* is still negative but very close to zero; when the reduced wind velocity is greater than eight A_2^* becomes positive and increase rapidly. Other flutter derivatives have no marked change at 0°, 3° and 5° attack angle but vary significantly at 7° attack angle.

(3) Comparison of the computed flutter onset speeds with the available ones obtained by the wind tunnel test shows that the errors of flutter critical wind velocity at different attack angles are less than 5%.

Attack Angle	Testing Case	reduced wind velocity (m/s)		error
		Test results	Calculation results	
0	case 1	6.13	6.29	2.61%
	case 2	10.36	10.78	3.89%
	case 3	12.64	12.98	2.62%
3	case 1	6.07	5.82	4.30%
	case 2	10.06	9.67	4.03%
	case 3	12.52	12.23	2.37%
5	case 1	5.78	5.97	3.18%
	case 2	7.92	8.08	1.98%
	case 3	8.55	8.87	3.60%
7	case 1	4.68	4.88	4.09%
	case 2	6.02	6.29	4.48%
	case 3	6.57	6.78	3.10%

Table 2. The error analysis of flutter critical velocity

Acknowledgments

This research was supported by the granted projects (NO.51308478, NO. 51678508 and NO. U1434205) from the China Natural Science Funding, and was supported by Major State Basic Research Development Program (NO. 2013CB036301) from China Ministry of Science and Technology.

References

[1] Scanlan R H and Tomko J J. Airfoil and bridges deck flutter derivatives [J]. J. Eng. Mech. Div. ， 1971，97（6）；1717~1733.

[2] Shinozuka M. Identification of linear structure dynamic system[J]. J. Eng . Mech. Div . ，1982,108(6)：1371-1390.

[3] Diana G, Cheli F, Zasso A, Collina A, Brownjohn J. Suspension bridge parameter identification in full scale test [J]. Journal of Wind Engineering and Industrial Aerodynamics, 1992, 41~44: 165~176.

[4] Noda M, Utsunomiya H, Nagao F, Kanda M, Shiraishi N. Effects of oscillation amplitude on aerodynamic derivatives [J]. Journal of Wind Engineering and Industrial Aerodynamics, 2003, 91: 101~111.

[5] Chen, X. Improved understanding of bimodal coupled bridge flutter based on closed-form solution [J]. Journal of Engineering Mechanics, 2007, 133(1): 22-31